DALTON
FULL PAPER

Influence of electron donor and acceptor substituents on the excited state properties of rhenium(I) tetracarbonyl chelate complexes

Frederik W. M. Vanhelmont,[a] Melath V. Rajasekharan,[a] Hans U. Güdel,*[,a] Silvia C. Capelli,[b] Jürg Hauser[b] and Hans-Beat Bürgi[b]

[a] *Departement für Chemie und Biochemie, Universität Bern, Freiestrasse 3, 3000 Bern 9, Switzerland. E-Mail: guedel@iac.unibe.ch*
[b] *Laboratorium für Chemische und Mineralogische Kristallographie, Universität Bern, Freiestrasse 3, 3000 Bern 9, Switzerland*

The new complexes $[Re(CO)_4(meppy)]$, $[Re(CO)_4(dmdcb)]PF_6$ and $[Re(CO)_4(dmeob)][CF_3SO_3]$ [Hmeppy = 3-methyl-2-phenylpyridine, dmdcb = 4,4′-di(methoxycarbonyl)-2,2′-bipyridine and dmeob = 4,4′-dimethoxy-2,2′-bipyridine] have been synthesized. The crystal and molecular structure of $[Re(CO)_4(meppy)]$ was determined by X-ray diffraction. High-resolution optical absorption, luminescence and Raman spectroscopy on single crystals and glasses at cryogenic temperatures revealed the lowest excited state for all complexes as a nominally $^3\pi$–π^* ligand centered state with some ^{1}MLCT character mixed in by spin–orbit coupling. This leads to the occurrence of metal–ligand vibrational sidebands in the absorption and luminescence spectra. The lowest excited state has a charge-transfer character of 1.7, 1.3 and 1.0% for $[Re(CO)_4(meppy)]$, $[Re(CO)_4(dmdcb)]PF_6$ and $[Re(CO)_4(dmeob)][CF_3SO_3]$, respectively. These results are compared with those for the unsubstituted complexes $[Re(CO)_4(ppy)]$ and $[Re(CO)_4(bpy)]PF_6$ (Hppy = 2-phenylpyridine and bpy = 2,2′-bipyridine). The influence of the σ-donor group on the energy of the excited states and on the mixing of ^{1}MLCT in the ^{3}LC state is negligibly small. π-Electron donor substituents increase the energy of the excited states and increase the singlet–triplet splittings; π-electron withdrawing groups have the opposite effect and increase the ^{1}MLCT character in the first excited state. The luminescence decay of $[Re(CO)_4(meppy)]$ is not single exponential due to a large inhomogeneous distribution of chromophores in the glass. This large distribution is due to the steric interaction of the methyl group with the phenyl part of the ligand.

1 Introduction

The $4d^6$ and $5d^6$ complexes containing π-accepting ligands have been synthesized and studied intensively by several physical methods[1,2] and still remain of interest[3] due to their photophysical and photochemical properties: they are important chromophores in photocatalysts and in solar energy conversion devices.[4,5] Studies on energy and electron transfer in dinuclear systems of these complexes were performed recently[6] and the charge separation in the excited state was determined.[7]

We concentrated on high-resolution optical spectroscopy of crystals and glasses of cyclometallated and chelated complexes of Rh^{III}, Ir^{III} and Re^{I} at cryogenic temperatures.[8–16] This is a very powerful technique for the investigation of excited state properties of these complexes. It provides information about vibronic coupling and energy splittings not available from low-resolution spectroscopy of glasses and solutions. The trend within the metal ion series mentioned above, and the influence of cyclometallation, was studied and interpreted.[16] The lowest excited state is a $^3\pi$–π^* ligand centered (LC) state with some metal to ligand charge transfer (^{1}MLCT) character mixed in by spin–orbit coupling in most of these complexes. The proximity of the first MLCT excitations is essential in determining the exact nature of the emitting state. It can be tuned by chemical and structural variation. It is known that adding electron-donating groups to the ligand increases the energy of the MLCT transition and the MLCT character in the lowest excited ^{3}LC state should therefore decrease. Electron-withdrawing groups should have the opposite effect.[17,18] However the influence of such substitutions on the nature of the emitting state has not been experimentally studied in detail.

In this paper we investigate the influence of σ and π substituents on the position of the transitions and on the mixing of ^{1}MLCT and ^{3}LC states. To this end we synthesized the following new complexes: $[Re(CO)_4(meppy)]$, $[Re(CO)_4(dmdcb)]PF_6$ and $[Re(CO)_4(dmeob)][CF_3SO_3]$, where $meppy^-$ = 3-methyl-2-phenylpyridinate [2-(3-methyl-2-pyridyl)phenyl], dmdcb = 4,4′-di(methoxycarbonyl)-2,2′-bipyridine and dmeob = 4,4′-dimethoxy-2,2′-bipyridine. The first complex contains the σ-electron donor methyl group, the second contains two π-electron withdrawing ester groups and the last two π-electron donor methoxy groups. We measured high-resolution optical spectra in order to investigate the excited state properties of the molecules mentioned above. Extended Hückel calculations were performed to identify the relevant one-electron excitations. The crystal structure of $[Re(CO)_4(meppy)]$ was determined in order to correlate the polarized single crystal absorption spectra with the molecular orientation in the crystal.

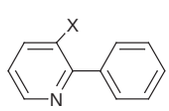

X = H Hppy
X = CH_3 Hmeppy

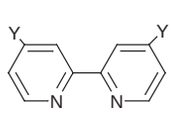

Y = H bpy
Y = OCH_3 dmeob
Y = $COOCH_3$ dmdcb

2 Experimental

2.1 Synthesis and characterization

3-Methyl-2-phenylpyridine was purchased from Aldrich and vacuum distilled prior to use; $[Re(CO)_4(meppy)]$ was prepared by the same synthetic route as that of $[Re(CO)_4(ppy)]$.[15] However an extra chromatography step with silica gel ($CHCl_3$–heptane 1:1) was necessary. The total yield was 12%. The yellow, plate-like crystals were grown by evaporation of the solvent from a diisopropyl ether solution of $[Re(CO)_4(meppy)]$. The

elemental analysis was performed by Novartis, Basel (Found: C, 42.19; H, 2.43; N, 3.00; O, 13.81. Calc.: C, 41.20; H, 2.16; N, 3.00; O, 13.72%). The IR spectrum of a 10^{-4} M solution of $[Re(CO)_4(meppy)]$ in CH_2Cl_2 showed maxima at 2088, 1985, 1967 and 1921 cm^{-1} in the region of the CO stretch vibrations.

4,4′-Di(methoxycarbonyl)-2,2′-bipyridine and 4,4′-dimethoxy-2,2′-bipyridine were synthesized according to literature methods.[19–21] The complex $[Re(CO)_4(dmdcb)]PF_6$ was prepared by a method analogous to the synthesis and crystallization of $[Re(CO)_4(bpy)]PF_6$ [13,22] with a small modification: the CH_2Cl_2 solution was refluxed for 18 h instead of stirred at room temperature for 8 h. The complex $[Re(CO)_4(dmdcb)]PF_6$ diluted in KBr showed maxima at 2126, 2027, 2008 and 1954 cm^{-1} in the CO stretch region; yellow-orange plate crystals (Found: C, 30.81; H, 1.97; F, 14.96; N, 4.04. Calc.: C, 30.22; H, 1.69; F, 15.93; N, 3.92%).

The complex $[Re(CO)_4(dmeob)][CF_3SO_3]$ was prepared by a method analogous to the synthesis of $[Re(CO)_4(bpy)][CF_3SO_3]$.[22] The white precipitate was filtered off, washed with CH_2Cl_2 and allowed to dry. The white powder was dissolved in acetonitrile. By slow evaporation of the solvent at room temperature very pale yellow diamond shaped crystals were obtained. The CO stretch vibrations of $[Re(CO)_4(dmeob)][CF_3SO_3]$ diluted in KBr were observed at 2118, 2020, 1997 and 1954 cm^{-1} (Found: C, 30.91; H, 1.92; F, 8.53; N, 4.18. Calc.: C, 30.77; H, 1.82; F, 8.59; N, 4.22%).

2.2 Crystal structure for $[Re(CO)_4(meppy)]$

Crystal data. $C_{16}H_{10}NO_4Re$, $M = 466.45$, orthorhombic, space group *Pbca*, $a = 12.349(1)$, $b = 12.966(1)$, $c = 19.607(1)$ Å, $U = 3139.4(4)$ Å^3, $T = 293(2)$ K, $Z = 8$, μ(Mo-Kα) = 7.757 mm^{-1}, 14 759 reflections collected, 3072 unique ($R_{int} = 0.0523$). Final $R1$ $[I > 2\sigma(I)] = 0.0323$ and $wR2$ $[I > 2\sigma(I)] = 0.0569$, $R1$ (all data) = 0.0622 and $wR2$ (all data) = 0.0648, goodness of fit on $F^2 = 1.308$.

CCDC reference number 186/1078.

See http://www.rsc.org/suppdata/dt/1998/2893/ for crystallographic files in .cif format.

2.3 Optical spectroscopy

The same experimental set-ups were used as for the measurements of $[Re(CO)_4(ppy)]$.[15] The 488 nm line of an Ion Laser Technology 5000 Ar^+ laser was used for the Raman spectrum. The 457.9 nm line of the same laser was used for the luminescence line narrowing (LLN) spectrum.

3 Results

3.1 Crystal structure

The complex $[Re(CO)_4(meppy)]$ crystallizes in a layer-like structure: layers of Re and COs interchange with layers of meppy. The largest crystal face is the $(\bar{1}03)$ plane and its longest edge coincides with the *b* axis. This crystal packing is completely different from that of $[Re(CO)_4(ppy)]$ and $[Re(CO)_4(thpy)]$ [$thpy^-$ = 2-(2-thienyl)pyridinate].[15,16] They crystallize in the monoclinic space group $P2_1/c$ with four molecules per unit cell.

The molecular structure is shown in Fig. 1. The Re–N distance is 0.030 Å longer than the Re–C^- distance. This difference is 0.024 Å in $[Re(CO)_4(ppy)]$.[15] The bite angle of $meppy^-$ is 75.0° as compared to 76.2° in $[Re(CO)_4(ppy)]$. The *trans* CO ligands show longer Re–C distances than the *cis* COs (1.989 and 1.997 *vs* 1.919 and 1.967 Å). Similar Re–C bond lengths are found in $[Re(CO)_4(ppy)]$ (1.976 and 1.981 *vs* 1.914 and 1.941 Å). The molecular structure is therefore comparable with that of $[Re(CO)_4(ppy)]$ except for the dihedral angle between the phenyl and the pyridine ring, which is 4.6(10)° in $[Re(CO)_4(meppy)]$ but only 1.1° in $[Re(CO)_4(ppy)]$. This difference is probably due to the steric repulsion of the methyl group and H(12).

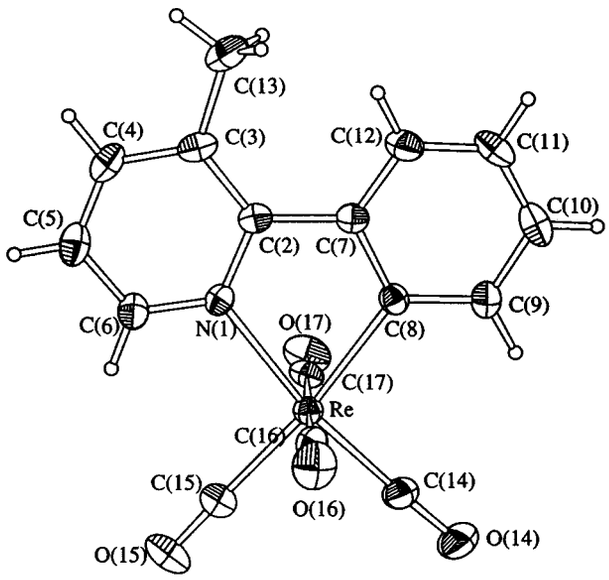

Fig. 1 An ORTEP[23] plot of a $[Re(CO)_4(meppy)]$ molecule (20% probability level for the thermal ellipsoids) with the atomic numbering scheme used in the text.

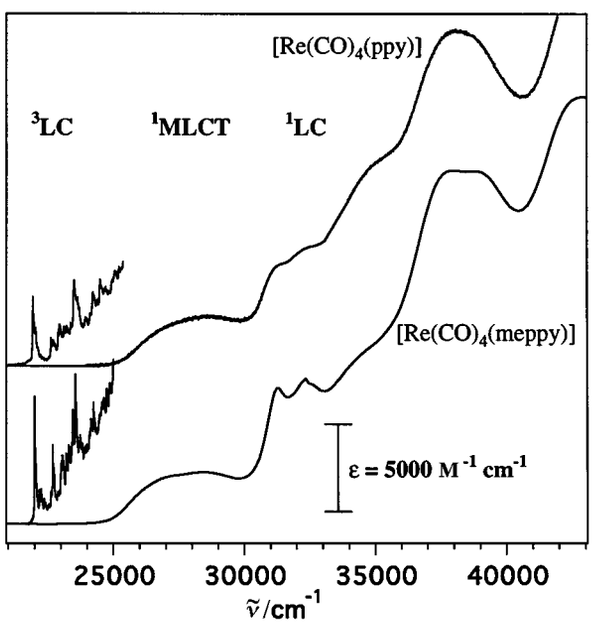

Fig. 2 The UV/VIS absorption spectra of 10^{-5} M solutions of $[Re(CO)_4(ppy)]$ and $[Re(CO)_4(meppy)]$ in CH_2Cl_2 at room temperature and single-crystal absorption spectra (scaled up by a factor 1000) of $[Re(CO)_4(ppy)]$ and $[Re(CO)_4(meppy)]$. Both crystal spectra were measured at 10 K.

3.2 Absorption spectra

The UV/VIS solution absorption spectrum of 10^{-5} M $[Re(CO)_4(meppy)]$ in CH_2Cl_2 at room temperature is shown in Fig. 2 (lower trace) together with the unpolarized absorption spectrum of a single crystal at 10 K. The corresponding spectra for $[Re(CO)_4(ppy)]$ are shown in the upper traces for comparison. Both crystal spectra are scaled up by a factor 1000. The observed transitions in the crystal spectra and their highly resolved fine structure were not observed in the solution spectra, since they are too weak and inhomogeneously broadened. The transitions above 25000 cm^{-1} could not be seen in the single crystal absorption spectrum due to their high intensity. The solution spectra of the two complexes are very similar.

The solution absorption spectra of $[Re(CO)_4(dmeob)]^+$, $[Re(CO)_4(bpy)]^+$ and $[Re(CO)_4(dmdcb)]^+$ are presented in Fig. 3, together with the unpolarized single crystal absorption

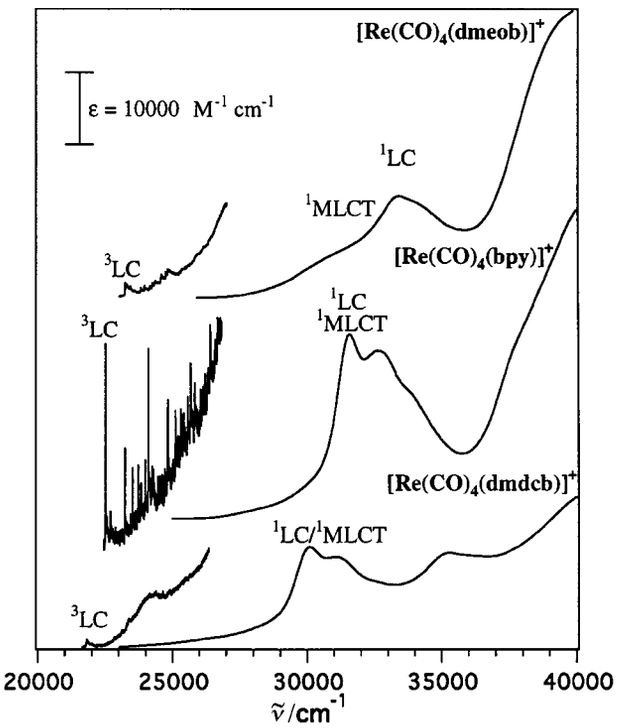

Fig. 3 The UV/VIS absorption spectra of a 10^{-5} M solution of [Re(CO)$_4$(dmeob)][CF_3SO_3] in acetonitrile (top) and of 10^{-5} M solutions of [Re(CO)$_4$(bpy)]PF_6 (middle) and [Re(CO)$_4$(dmdcb)]PF_6 in CH_2Cl_2 at room temperature, supplemented by the unpolarized single-crystal absorption spectra (scaled up by a factor of 500, 50 and 250, respectively) at 10 K.

spectra at 10 K (scaled up by a factor of 500, 50 and 250, respectively). The transitions above 28000 cm^{-1} were too intense and inhomogeneously broadened to be observed in the crystal spectra, whereas the transitions observed in the crystal spectra were too weak to be detected in the solution spectra. Both the intense transitions and the weak absorptions show a blue-shift on increasing the electron donor strength of the substituents.

The single crystal absorption spectra of [Re(CO)$_4$(dmeob)][CF_3SO_3] and [Re(CO)$_4$(dmdcb)]PF_6 are more inhomogeneously broadened than the spectrum of [Re(CO)$_4$(bpy)]PF_6 (Fig. 3). The fine structure is due to vibrational sidebands, overtones and combination bands built on electronic origins at 21 823 and 23 250 cm^{-1} for [Re(CO)$_4$(dmdcb)]PF_6 and [Re(CO)$_4$(dmeob)][CF_3SO_3], respectively. The vibrational sideband structure is very similar to that of [Re(CO)$_4$(bpy)]PF_6 (Fig. 3 and ref. 13).

A comparison of the crystal absorption spectra of the two cyclometallated complexes is presented on an expanded scale in Fig. 4. These two spectra also show a resemblance, with the fine structure better resolved for [Re(CO)$_4$(meppy)] due to a smaller inhomogeneous broadening. The observed fine structure is due to vibrational sidebands, combination bands and overtones built on the electronic origins at 21 938 and 22 000 cm^{-1} for [Re(CO)$_4$(ppy)] and [Re(CO)$_4$(meppy)], respectively. The fundamental vibrations are indicated in Fig. 4. Corresponding vibrational sidebands are at slightly higher energy for [Re(CO)$_4$(meppy)] than for [Re(CO)$_4$(ppy)], except for the ring breathing mode which is at 1551 *vs.* 1563 cm^{-1}, respectively. The metal–ligand vibrations are observed at 181 and 259 cm^{-1} for [Re(CO)$_4$(meppy)], whereas a metal–ligand vibrational sideband is found at 99 cm^{-1} for [Re(CO)$_4$(ppy)].[15] Polarized single-crystal absorption spectra [light propagation perpendicular to the largest crystal face ($\bar{1}03$)] of [Re(CO)$_4$(meppy)] show an intensity ratio of $I_{\perp b} : I_{\parallel b} = 8 : 1$ throughout the crystal spectrum.

3.3 Luminescence and Raman spectra

3.3.1 Cyclometallated complexes. The luminescence spectrum

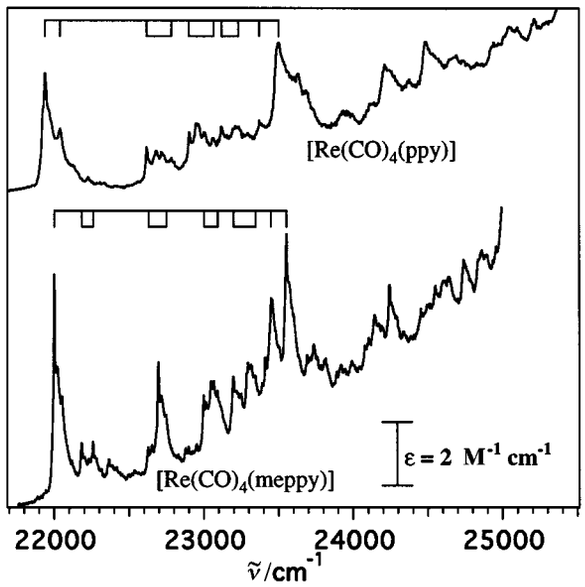

Fig. 4 Single-crystal absorption spectra of [Re(CO)$_4$(ppy)] and [Re(CO)$_4$(meppy)]. Both spectra were measured at 10 K. The fundamental vibrations of both complexes are indicated.

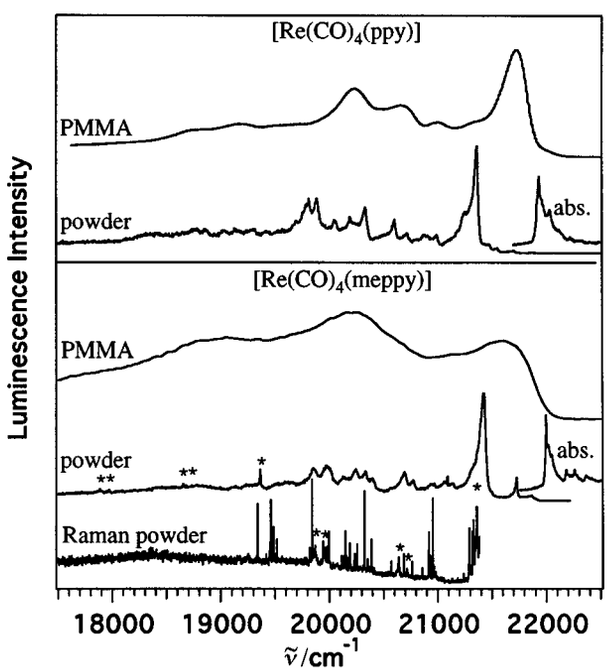

Fig. 5 Luminescence spectra of [Re(CO)$_4$(meppy)] and [Re(CO)$_4$(ppy)] in the crystalline state and dissolved in a poly(methylmethacrylate) (PMMA) glass (10^{-4} M). The Raman spectrum of crystalline [Re(CO)$_4$(meppy)] is displayed relative to the origin of the major trap. The luminescent trap at 19 363 cm^{-1} and its sidebands (all indicated by asterisks) are also excited in the Raman spectrum. All spectra were measured at 10 K.

of polycrystalline [Re(CO)$_4$(meppy)] at 10 K is shown at the bottom of Fig. 5. The luminescence is red-shifted with respect to the absorption origin which is included for comparison. The fine structure is due to vibrational sidebands built on electronic origins at 21 866, 21 728, 21 430 and 19 363 cm^{-1}. At higher temperatures the features get broader and only the luminescence built on the 19 363 cm^{-1} origin persists. All these luminescences are due to traps in the crystal. The origin at 21 430 cm^{-1} and its sidebands are broader than the origins at 21 728 and 19 363 cm^{-1}. These differences are due to different degrees of inhomogeneous broadening, reflecting the environment of the trap site in the crystal. The powder luminescence spectrum of [Re(CO)$_4$(ppy)] at 10 K is given for comparison in

Fig. 5. It is also a trap emission with a rich fine structure. It mainly consists of vibrational sidebands built on the electronic origin at 21 366 cm^{-1}. At higher energy some origins with very low intensity are observed. At higher temperatures the fine structure fades out and the intensity decreases. The luminescence spectra of both crystalline $[Re(CO)_4(ppy)]$ and $[Re(CO)_4(meppy)]$ thus originate from shallow traps. A deeper trap (19 363 cm^{-1}) dominates the luminescence of $[Re(CO)_4(meppy)]$ at higher temperatures.

The luminescence spectra of $[Re(CO)_4(ppy)]$ and $[Re(CO)_4(meppy)]$ diluted in a PMMA film are also presented in Fig. 5. The fine structure is much less resolved than in the crystal spectra, which is a result of inhomogeneous broadening. The inhomogeneous broadening is larger for $[Re(CO)_4(meppy)]$ than for $[Re(CO)_4(ppy)]$ dissolved in PMMA. In contrast to $[Re(CO)_4(ppy)]$,[15] we were unsuccessful in luminescence line narrowing the spectrum of $[Re(CO)_4(meppy)]$ in PMMA.

The Raman spectrum of crystalline $[Re(CO)_4(meppy)]$ at 10 K is presented in Fig. 5 relative to the electronic origin of the major trap. Most of the Raman intensity occurs within 1600 cm^{-1}, *i.e.* the region of fundamental vibrational sidebands in the absorption and luminescence spectra. A one-to-one correlation of the Raman lines with the vibrational sidebands was not attempted because of the very large number of modes and their very different relative intensities in the two processes. The prominent Raman lines between 1900 and 2100 cm^{-1} are conspicuously absent in the vibrational sideband structure of the optical transitions. They are due to CO stretch vibrations, and we immediately conclude that their coupling to the electronic transitions is negligible. The luminescent trap with origin at 19 363 cm^{-1} is excited with the 488 nm line of the Ar^+ laser. This trap luminescence is marked by asterisks in Fig. 5.

The luminescence decay curves of $[Re(CO)_4(ppy)]$ and $[Re(CO)_4(meppy)]$ display a deviation from single exponential decay. However, for $[Re(CO)_4(ppy)]$ this deviation is small and we can derive an average lifetime of 89 ± 5 μs. For $[Re(CO)_4(meppy)]$ we determined the slope of the data in two time windows: between 0 and 30 μs and between 500 μs and 1 ms, respectively. The lifetime increases from 53 to 123 μs between these windows at 20 K. Above 100 K both the lifetime and the intensity of the luminescence of $[Re(CO)_4(meppy)]$ in PMMA drop as a result of non-radiative relaxation processes. The luminescence decay curve of the major trap at 21 430 cm^{-1} in the crystal luminescence spectrum of $[Re(CO)_4(meppy)]$ at 10 K deviates from single exponential decay too. Between 500 μs and 1 ms we derive a lifetime of 81 μs, well within the range of lifetimes determined under the same conditions in the PMMA glass.

3.3.2 Diimine complexes. The powder luminescence spectra of $[Re(CO)_4(dmeob)][CF_3SO_3]$, $[Re(CO)_4(bpy)]PF_6$ and $[Re(CO)_4(dmdcb)]PF_6$ at 10 K are presented in Fig. 6. The luminescences are red-shifted with respect to the absorption origins. The fine structure in the spectrum of $[Re(CO)_4(dmeob)][CF_3SO_3]$ is due to vibrational sidebands built on electronic origins at 23 128 and 22 900 cm^{-1}. The luminescence spectrum of $[Re(CO)_4(bpy)]PF_6$ is discussed in ref. 13. At higher temperatures the fine structure in the powder luminescence spectrum of $[Re(CO)_4(dmeob)][CF_3SO_3]$ and $[Re(CO)_4(bpy)]PF_6$ fades out and the intensity decreases. The luminescence is therefore due to luminescent traps in the crystalline material. In contrast to $[Re(CO)_4(bpy)]^+$ and $[Re(CO)_4(dmeob)]^+$ compounds, the luminescence spectrum of crystalline $[Re(CO)_4(dmdcb)]PF_6$ at 10 K shows a broad luminescence which is strongly red-shifted with respect to the absorption origin. This luminescence is discussed in section 4.1.

The luminescence spectra of $[Re(CO)_4(dmeob)][CF_3SO_3]$, $[Re(CO)_4(bpy)]PF_6$ and $[Re(CO)_4(dmdcb)]PF_6$ in different glasses at 10 K are presented in Fig. 6. They show inhomogeneously broadened luminescence with a similar structure to that

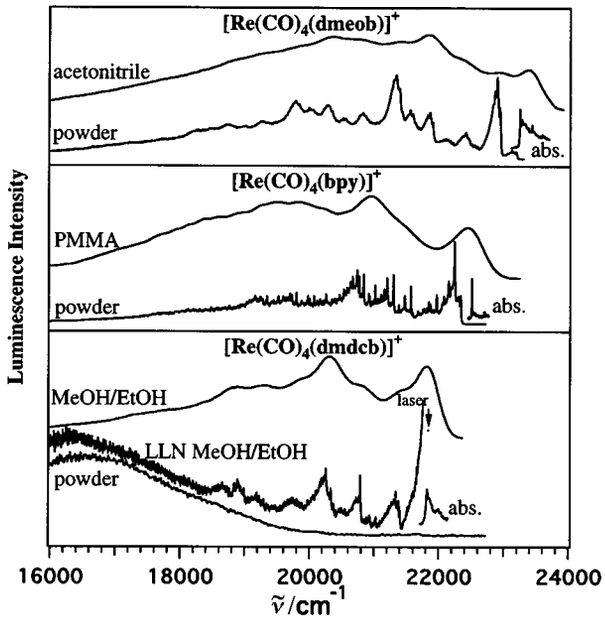

Fig. 6 Luminescence spectra of crystalline $[Re(CO)_4(dmeob)][CF_3SO_3]$, $[Re(CO)_4(bpy)]PF_6$ and $[Re(CO)_4(dmdcb)]PF_6$ and dissolved in acetonitrile, PMMA and MeOH–EtOH, respectively. The luminescence line narrowed (LLN) spectrum of $[Re(CO)_4(dmdcb)]PF_6$ in MeOH–EtOH is shown. The arrow indicates the position of the exciting laser line. The absorption origins of the crystal spectra are included for comparison. All spectra were registered at 10 K.

of the powder spectra. We were able to luminescence line narrow the $[Re(CO)_4(dmdcb)]PF_6$ spectrum. The luminescence of $[Re(CO)_4(dmdcb)]^+$ in EtOH–MeOH sharpens in the region above 20 000 cm^{-1}. Below 20 000 cm^{-1} a broad luminescence is observed, similar to the luminescence observed in the powder.

The luminescence decay curves are single exponential at 10 K with τ = 32, 32 and 52 μs for $[Re(CO)_4(dmdcb)]PF_6$, $[Re(CO)_4(bpy)]PF_6$[13] and $[Re(CO)_4(dmeob)][CF_3SO_3]$, respectively. Above 150 K strong intensity and lifetime drops due to non-radiative relaxation processes are observed.

3.4 Extended Hückel calcultions

We carried out extended Hückel calculations for all the presented complexes using the CACAO program by Mealli and Proserpio.†[24] The atomic positions found in the crystal structure determinations (see section 3.1 and ref. 13) and typical bond distances and angles for the substituents were used for the calculation. The cyclometallating and chelating ligands were chosen to be completely planar, to ensure C_s or C_{2v} molecular symmetry.

The results of the calculation for $[Re(CO)_4(meppy)]$ are shown on the right-hand side of Fig. 7. The LUMO, HOMO and the three orbitals just below with substantial rhenium d character (35, 45 and 46% with decreasing energy, respectively) are shown with their relative energy. Both the HOMO and LUMO are essentially $meppy^-$ centered π orbitals (2 and 0% metal character, respectively). Therefore the lowest energy transition in this one-electron picture is expected to be a LC transition, with the first MLCT transition about 6000 cm^{-1} higher in energy, see Fig. 7.

A comparison with the left side of Fig. 7 shows that all the orbitals are very similar in $[Re(CO)_4(ppy)]$ and $[Re(CO)_4$-

† The following valence orbital ionization energies (eV, *ca* 1.60×10^{-19} J) were used in the calculation: C 2s −21.4, 2p −11.4; H 1s −13.6; N 2s −26.0, 2p −13.4; O 2s −32.3, 2p −14.8;[25] Re 6s −9.36, 6p −5.96, 5d −12.66.[26]

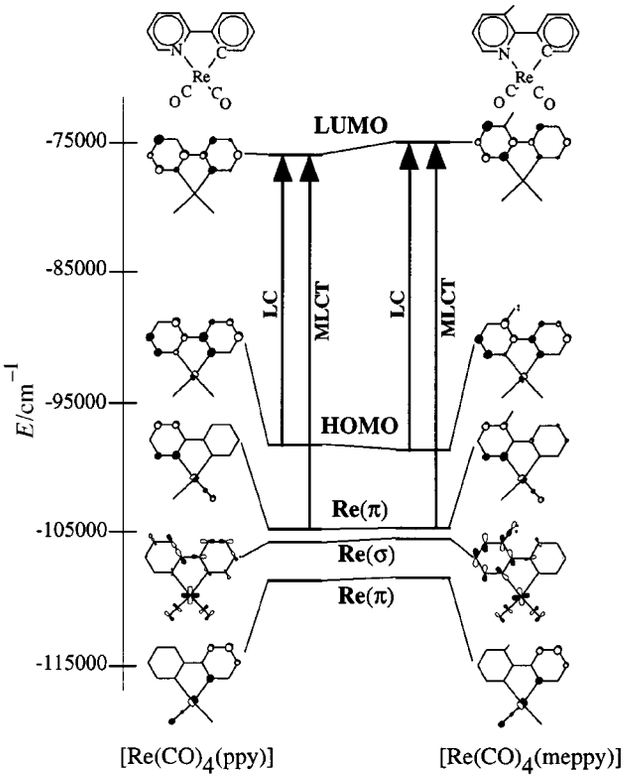

Fig. 7 Results of the extended Hückel calculations for $[Re(CO)_4(ppy)]$ and $[Re(CO)_4(meppy)]$. The HOMO, LUMO and nominal metal orbitals are shown together with the relevant one-electron excitations. The contribution of the out-of-plane COs is omitted to prevent confusion with the rhenium contribution.

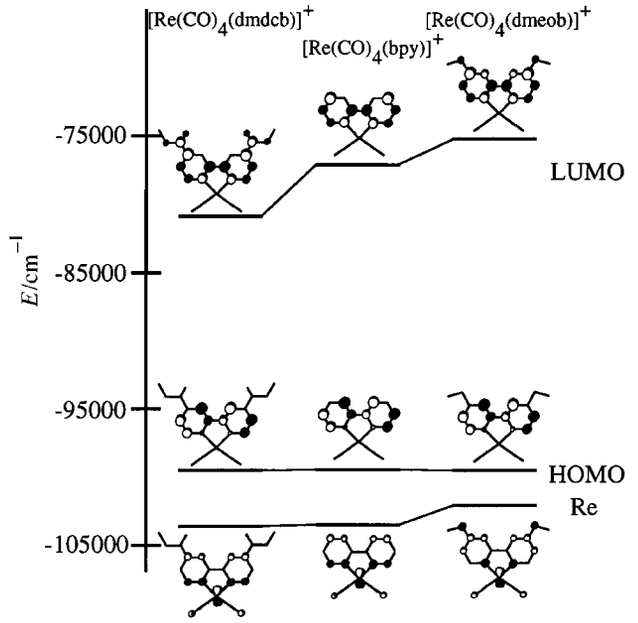

Fig. 8 Results of the extended Hückel calculations for $[Re(CO)_4(dmdcb)]^+$, $[Re(CO)_4(bpy)]^+$ and $[Re(CO)_4(dmeob)]^+$. The wavefunctions and their respective energies for the LUMO, HOMO and the highest-energy nominal metal orbital are shown. The contribution of the out-of-plane COs is omitted to prevent confusion with the rhenium contribution.

(meppy)], except for the σ-metal orbital in which an electron density redistribution occurs. In $[Re(CO)_4(ppy)]$ the electron density is distributed over Re, the COs and the whole ppy^- ligand, whereas in $[Re(CO)_4(meppy)]$ the phenyl ring loses electron density. The LC transition is expected to be about 1200 cm^{-1} and the MLCT transition about 800 cm^{-1} higher in energy for $[Re(CO)_4(meppy)]$ in comparison with the non-methylated $[Re(CO)_4(ppy)]$.

The results of the extended Hückel calculations for $[Re(CO)_4(dmeob)]^+$, $[Re(CO)_4(bpy)]^+$ and $[Re(CO)_4(dmdcb)]^+$ are presented in Fig. 8. The LUMO, HOMO and the highest lying filled π orbital with substantial metal character {48, 47 and 31% for $[Re(CO)_4(dmdcb)]^+$, $[Re(CO)_4(bpy)]^+$ and $[Re(CO)_4(dmeob)]^+$, respectively} are given with their respective energies. Both the HOMO and LUMO are diimine centered (0% metal character), whereas the metal orbital lies lower in energy. Therefore the LC transitions are expected at lower energies than the MLCT transitions. The LUMO contains a substantial substituent contribution and therefore its energy position is strongly influenced by the substitutions. Adding π-electron withdrawing groups decreases the energy of the LUMO and π-electron donating substituents have the opposite effect. The same trend (although weaker) is found for the metal orbitals, see Fig. 8. The π substituents have no influence on the HOMO. This is in contrast with the σ-electron donor methyl group. It decreases the energy of the HOMO slightly and influences the energies of the metal orbitals only to a minor extent, see Fig. 7.

4 Discussion

4.1 Assignment of the excited states

By comparison with the corresponding spectra of $[Re(CO)_4(ppy)]$,[15] $[Re(CO)_4(bpy)]^+$ [13] and the free heterocycles,[27] it is possible to assign the observed transitions in the absorption spectra presented in Figs. 2, 3 and 4. The bands above 31 000 cm^{-1} in the spectra of the cyclometallated species and above 28 000 cm^{-1} for the diimine complexes are assigned as ^{1}LC transitions. The band with maximum around 28 500 cm^{-1} in the solution absorption spectrum of $[Re(CO)_4(meppy)]$ and $[Re(CO)_4(ppy)]$ is due to a ^{1}MLCT transition. The corresponding transition is masked by the more intense ^{1}LC transition in the absorption spectra of $[Re(CO)_4(bpy)]^+$ and $[Re(CO)_4(dmdcb)]^+$. The ^{1}MLCT transition is observed in the spectrum of $[Re(CO)_4(dmeob)]^+$ as a shoulder around 31 500 cm^{-1}.

The highly structured absorption bands at low energy which were only observed in the crystal spectra are due to ^{3}LC excitations in all the complexes studied here. They consist of vibrational sidebands and their combination bands and overtones built on electronic origins at 22 000, 21 823 and 23 250 cm^{-1} for $[Re(CO)_4(meppy)]$, $[Re(CO)_4(dmdcb)]^+$ and $[Re(CO)_4(dmeob)]^+$, respectively. The fundamental vibrations of $[Re(CO)_4(meppy)]$ are indicated in Fig. 4. The sidebands are all due to ligand vibrations, except the bands at 181 and 259 cm^{-1} in the $[Re(CO)_4(meppy)]$ spectrum, at 171 cm^{-1} in the $[Re(CO)_4(dmdcb)]^+$ spectrum and at 187 cm^{-1} in the $[Re(CO)_4(dmeob)]^+$ spectrum. These vibrations are discussed in the next section. The apparent broad band around 24 000 cm^{-1} in the absorption spectrum of $[Re(CO)_4(dmdcb)]PF_6$ is probably the result of inhomogeneous broadening of the vibrational sidepeaks. The first ^{3}MLCT transition is expected at higher energy.

The luminescence lifetimes, $\tau[Re(CO)_4(meppy)] = 53–123$, $\tau[Re(CO)_4(dmdcb)^+] = 32$ and $\tau[Re(CO)_4(dmeob)^+] = 52$ μs and the oscillator strengths $f(^3LC) = 4.3 \times 10^{-5}$, 1×10^{-4} and 5×10^{-5} for $[Re(CO)_4(meppy)]$, $[Re(CO)_4(dmdcb)]^+$ and $[Re(CO)_4(dmeob)]^+$, respectively, are in good accord with a ^{3}LC assignment of the emitting state. The corresponding values for $[Os(bpy)_3]^{2+}$, for which a ^{3}MLCT assignment has been made for the first excited state, are $\tau = 1.8$ μs and $f(^3MLCT) = 4 \times 10^{-4}$.[28,29]

The vibrational sideband structures of the major trap in the luminescence spectrum of crystalline $[Re(CO)_4(meppy)]$ and the single crystal absorption spectrum are very similar (see Figs. 4 and 5) and obviously due to $meppy^-$ vibrational modes. The absence of CO modes in the vibrational sideband structure

Table 1 Excited state quantities for the studied complexes

	$[Re(CO)_4(ppy)]$[a]	$[Re(CO)_4(meppy)]$	$[Re(CO)_4(dmdcb)]^+$	$[Re(CO)_4(bpy)]^+$[a]	$[Re(CO)_4(dmeob)]^+$
$f(^3LC)$	4.2×10^{-5}	4.3×10^{-5}	1×10^{-4}	7×10^{-5}	5×10^{-5}
$f(^1MLCT)$	5.7×10^{-2}	5.7×10^{-2}	2.5×10^{-1}	4×10^{-1}	2.2×10^{-1}
$\tilde{\nu}(^3LC)(origin)/cm^{-1}$	21 938	22 000	21 823	22 510	23 250
$\tilde{\nu}(^1MLCT)(max.)/cm^{-1}$	28 500	28 500	31 000[b]	31 700[b]	31 500
$\tilde{\nu}(^1LC)(max.)/cm^{-1}$	31 260	31 240	30 110	31 570	33 660
$\Delta E(max.)$[c]$/cm^{-1}$	4 762	4 700	6 490	7 260	7 580
$\langle ^3LC\|H_{so}\|^1MLCT\rangle/cm^{-1}$	81	82	85	63	76
$\tau_{exp}/\mu s$	89	53–123	32	32	52
τ_{rad}[d]$/\mu s$	74	72	31	42	55
α[e]	0.017	0.017	0.013	0.009	0.010

[a] The values for $[Re(CO)_4(ppy)]$ and $[Re(CO)_4(bpy)]^+$ are taken from ref. 16. [b] Estimated. [c] It is important to use the maxima of the overall absorption bands for the calculation of ΔE. [d] As defined in formula (4). [e] As defined in formula (3).

confirms the essentially meppy$^-$ centered character of the lowest-energy excitation. The same is observed in the luminescence spectra of crystalline $[Re(CO)_4(bpy)]^+$ and $[Re(CO)_4(dmeob)]^+$ (Fig. 6). The crystal of $[Re(CO)_4(dmdcb)]^+$, on the other hand, shows a broad unstructured luminescence band. We tentatively assign it to a ^{3}MLCT luminescence of a rhenium tricarbonyl impurity which is being excited by energy transfer from the bulk. The luminescence of this impurity is also observed in the spectrum of a MeOH–EtOH glass at 10 K when excited at 21 839 cm^{-1}. The ^{3}LC luminescence of the main species is partially narrowed under these conditions (see LLN trace in Fig. 6).[30] When the same sample is broad band excited in the UV at 10 K, however, the inhomogeneously broadened ^{3}LC emission of the main species is observed. The sideband structure is due to diimine vibrations, typical of a $^3\pi$–π^* transition.

Also the extended Hückel calculations predict a π–π^* ligand centered transition as lowest energy transition with the first MLCT excitation about 6000, 4100 and 2600 cm^{-1} higher in energy for $[Re(CO)_4(meppy)]$, $[Re(CO)_4(dmdcb)]^+$ and $[Re(CO)_4(dmeob)]^+$, respectively. Extended Hückel calculations do not consider electron–electron repulsion and the resulting singlet–triplet splittings; ^{1}MLCT–^{3}MLCT splittings are typically of the order of 2000–4000 cm^{-1}, whereas ^{1}LC–^{3}LC splittings are of the order of 10 000 cm^{-1}. We conclude that a ^{3}LC state is expected to be the lowest excited state for all the studied complexes.

4.2 MLCT Character in the first excited state

There are several indications of some charge transfer character in this nominally ^{3}LC state: Re–meppy and Re–diimine vibrations are observed in the single-crystal absorption spectra at 181 and 259 cm^{-1} for $[Re(CO)_4(meppy)]$, at 171 cm^{-1} for $[Re(CO)_4(dmdcb)]^+$ and at 187 cm^{-1} for $[Re(CO)_4(dmeob)]^+$ (Figs. 3 and 4). The Raman peak at 96 cm^{-1} is also assigned as a Re–meppy vibration (Fig. 5). This vibration is also present as a shoulder in the luminescence spectrum of crystalline $[Re(CO)_4(meppy)]$. The vibrations at 172 cm^{-1} in the luminescence line narrowed spectrum of $[Re(CO)_4(dmdcb)]^+$, and at 165 cm^{-1} in the powder luminescence spectrum of $[Re(CO)_4(dmdcb)]^+$, are Re–diimine vibrations too (Fig. 6).

Metal–ligand vibrations are typical for transitions bearing some MLCT character and their intensity is a measure for the changes in the corresponding metal–ligand bonding induced by the electronic excitation. However, there is no reliable technique to determine a quantitative value of the charge-transfer character in the emitting state from the intensity of the metal–ligand vibrations, and we use the luminescence lifetimes and the oscillator strengths found in the absorption spectra for an estimate.

It is possible to describe the mixing of the ^{1}MLCT into the ^{3}LC state quantitatively by second-order spin–orbit coupling perturbation theory as suggested by Komada *et al.*[31] We have used this model before for other $4d^6$ and $5d^6$ complexes.[9–11] The spin–orbit coupling matrix element is given by eqn. (1) where

$$\langle ^3LC|H_{so}|^1MLCT\rangle = \sqrt{\frac{1}{3}\frac{f(^3LC)}{f(^1MLCT)}\frac{\nu(^1MLCT)}{\nu(^3LC)}}\Delta E \quad (1)$$

$f(^3LC)$ and $f(^1MLCT)$ are the oscillator strengths of the ^{3}LC and ^{1}MLCT transitions, respectively, and $\nu(^3LC)$ and $\nu(^1MLCT)$ are the corresponding frequencies; ΔE is the energy difference between the maxima of the corresponding absorption bands and the factor 1/3 accounts for the different spin multiplicities. Inserting the values derived from Figs. 2, 3 and 4 we obtain for $\langle ^3LC|H_{so}|^1MLCT\rangle$ values of 82, 85 and 76 cm^{-1} for $[Re(CO)_4(meppy)]$, $[Re(CO)_4(dmdcb)]^+$ and $[Re(CO)_4(dmeob)]^+$, respectively.‡ The corresponding values are 81 cm^{-1} for $[Re(CO)_4(ppy)]$ and 63 cm^{-1} for $[Re(CO)_4(bpy)]^+$.[16] The charge transfer character in the first ^{3}LC state is described by the quantity α; eqns. (2) and (3). We obtain values for α of 0.017, 0.013 and

$$\Psi_{exc} = \sqrt{1-\alpha^2}|^3LC\rangle + \alpha|^1MLCT\rangle \quad (2)$$

$$\alpha = \langle ^3LC|H_{so}|^1MLCT\rangle/\Delta E \quad (3)$$

0.010 for $[Re(CO)_4(meppy)]$, $[Re(CO)_4(dmdcb)]^+$ and $[Re(CO)_4(dmeob)]^+$, respectively. The corresponding values for $[Re(CO)_4(ppy)]$ and $[Re(CO)_4(bpy)]^+$ are 0.017 and 0.009, respectively.[16] All these values are listed in Table 1 for a comprehensive comparison. The admixture of the ^{1}MLCT in the ^{3}LC state should lead to an increase of the zero field splitting of the triplet state.[31] However it is too small to be resolvable with the techniques used in this study. More advanced techniques, such as resonant luminescence line narrowing and Zeeman experiments,[32] could possibly resolve the zero field splitting.

The luminescence lifetimes at 10 K are about three orders of magnitude shorter than the lifetime of the free heterocycle,§ see Table 1. An estimate of the radiative lifetime of the first excited state is obtained by using formula (4), where f is the

$$\tau_{rad} = 1.5 \times 10^4 \left(\frac{1}{f}\right)\frac{(c/\nu)^2}{n[(n^2+2)/3]^2}\frac{g_e}{g_g} \quad (4)$$

oscillator strength, c the velocity of light, ν the transition frequency, n the refractive index and g_e and g_g are the degeneracies of the excited and ground state, respectively. Choosing $n = 1.5$ we calculate $\tau_{rad} = 72$, 31 and 55 μs for $[Re(CO)_4(meppy)]$, $[Re(CO)_4(dmdcb)]^+$ and $[Re(CO)_4(dmeob)]^+$, respectively. These values are in excellent agreement with the experimentally

‡ For the $[Re(CO)_4(diimine)]^+$ complexes the ^{1}MLCT and ^{1}LC transitions (almost) coincide. In formula (1) we have therefore taken for $f(^1MLCT)$ the sum of the oscillator strengths of the two singlet transitions and for the frequency we used an effective frequency. We have made this assumption before for $[Re(CO)_4(bpy)]^+$, see ref. 16.

§ We expect the luminescence lifetime of meppy to be in the same order of magnitude as that of ppy, namely $\tau > 0.1$ s.[33]

observed lifetimes, see Table 1, and we conclude that the luminescence lifetimes are completely radiative at low temperatures.

The polarized single-crystal absorption spectrum provides a most elegant way to demonstrate that the intensity of the lowest-energy electronic excitation has its origin in the MLCT character mixed into the ^{3}LC state. From the experimentally determined absorption intensity ratios for different polarizations and the known orientation of the molecules in the crystal it is possible to derive the principal axes of the transition moment within the molecule. This procedure has been applied previously to other chelate complexes of d^6 ions[8–10,13,15,16] and is described in detail in ref. 8. The transition moment to the emitting state was invariably found to lie in the plane of the chelate ligand, and in the cyclometallated complexes to be tilted towards the pyridine side of the ligand. In the present study we employed this technique to the polarized absorption spectrum of [Re(CO)$_4$(meppy)] making use of the crystal structure information. The measured dichroic ratio $I_{\perp b} : I_{\parallel b} = 8 : 1$ is consistent with a transition moment polarized in the plane of the meppy$^-$ ligand and lying roughly parallel to the Re–C(2) direction, see Fig. 1. This result is significant. In free bpy, phen and, by analogy, similar compounds with conjugated π systems, the first ^{3}π–π* excitation is polarized out-of-plane.[34] The observed in-plane polarization in the complex is a strong indication that the ^{3}π–π* excitation intensity has another source than in the free heterocycle. The first MLCT transition is in-plane polarized, and using the so-called transition charge density method[35] it can be calculated from the extended Hückel wavefunctions Re(π) and LUMO connected by an arrow in Fig. 7. The direction thus obtained is approximately the Re–N direction, thus slightly overestimating the tilt towards the pyridine side of the ligand. Similar results were obtained for the cyclometallated $4d^6$ and $5d^6$ complexes [Re(CO)$_4$(ppy)], [Re(CO)$_4$(thpy)], [Rh(ppy)$_2$(bpy)]$^+$, [Rh(thpy)$_2$(bpy)]$^+$, [Ir(ppy)$_2$(bpy)]$^+$ and [Ir(thpy)$_2$(bpy)]$^+$.[8–10,13,15,16]

4.3 Influence of the substituents

4.3.1 σ-Donor substituent. Both the absorption and luminescence spectra of [Re(CO)$_4$(ppy)] and [Re(CO)$_4$(meppy)] are very similar (Figs. 2, 4 and 5). An analogous result was found by Watts and co-workers[36] on going from [Ir(ppy)$_2$(bpy)]$^+$ to [Ir(meppy)$_2$(bpy)]$^+$. The electronic origin of the ^{3}LC state moves from 21 938 to 22 000 cm^{-1} under methylation. This small blue-shift is qualitatively reproduced by the extended Hückel calculation (Fig. 7). Corresponding vibrational sidebands are at slightly higher energy for [Re(CO)$_4$(meppy)] than for [Re(CO)$_4$(ppy)] except for the ring breathing mode which is at 1551 *vs* 1563 cm^{-1}, respectively (see Fig. 4). The metal–ligand vibrations at 181 and 259 cm^{-1} in the single-crystal absorption spectrum of [Re(CO)$_4$(meppy)] are not observed in the corresponding spectrum of [Re(CO)$_4$(ppy)]. This might be due to the higher inhomogeneous broadening in the [Re(CO)$_4$(ppy)] spectrum or the peaks may be coinciding with the first and second overtone of the 99 cm^{-1} metal–ligand vibration of the non-methylated species.[15]

The luminescence decay curves of [Re(CO)$_4$(meppy)] at 20 K show a significant deviation from single exponentials. We ascribe this to a larger distribution of dihedral angles between the two aromatic rings in the [Re(CO)$_4$(meppy)] PMMA glass. In contrast to the other complexes in which the distribution is centered around a dihedral angle of zero, the steric effect of the methyl group favors a distorted conformation in [Re(CO)$_4$(meppy)] (see the crystal structure) and, as a result, an overall broader inhomogeneous distribution. This is also reflected in the larger bandwidth of the [Re(CO)$_4$(meppy)] PMMA luminescence spectrum in Fig. 5.

The luminescence spectra of the pure crystalline materials are dominated by traps at all temperatures. This is not unexpected for neutral molecular species with no shielding by counter ions in the crystal lattice.[16] For both [Re(CO)$_4$(ppy)] and [Re(CO)$_4$(meppy)] the emissions originating between 21 000 and 22 000 cm^{-1} are assigned to traps consisting of [Re(CO)$_4$(ppy)] and [Re(CO)$_4$(meppy)] molecules in defect crystal sites, respectively. For [Re(CO)$_4$(meppy)] there is a considerably deeper trap at 19 363 cm^{-1} with a different sideband structure, which must have a different origin. This suggests a defect molecule rather than a lattice defect as the origin of the trap. It is well known that tricarbonyl complexes of Re$^+$ are very stable luminescent species. Most of these are ^{3}MLCT emitters, but ^{3}π–π* emission originating at about 21 700 cm^{-1} has been reported for [Re(CO)$_3$(phen)(CH$_3$CN)]$^+$.[37] The most probable contamination is a [Re(CO)$_3$(meppy)Cl]$^-$ species, since the [Re(CO)$_5$Cl] complex is the starting material for the synthesis of [Re(CO)$_4$(meppy)]. An extended Hückel calculation on [Re(CO)$_3$(meppy)Cl]$^-$ results in a HOMO − LUMO gap which is 1000 cm^{-1} smaller in energy in comparison with the tetracarbonyl complex.[38] We conclude that a minute contamination by a tricarbonyl complex is most likely responsible for the 19 363 cm^{-1} trap emission in [Re(CO)$_4$(meppy)].

The ^{1}MLCT absorption band position is hardly influenced by the methylation (see Fig. 2 and Table 1), although the extended Hückel calculation predicts a slight increase of about 800 cm^{-1} (Fig. 7). The MLCT character in the ^{3}LC state is unchanged (section 4.2 and Table 1). All orbitals and their respective energies are very similar in [Re(CO)$_4$(ppy)] and [Re(CO)$_4$(meppy)], except the rhenium(σ) orbital (Fig. 7). In [Re(CO)$_4$(meppy)] there is a higher electron density in the pyridine ring than in the equivalent orbital of [Re(CO)$_4$(ppy)]. This is due to the σ-donor character of the methyl group. However, this metal orbital is not involved in the spectroscopically relevant transitions of the present study, which are indicated with arrows in Fig. 7. The Re(σ) ⟶ π* transition is symmetry forbidden in first order and therefore the lowest energy ^{3}π ⟶ π* transition cannot steal intensity from this transition. The influence of methylation of the pyridine ring on the luminescence properties is therefore very small.

4.3.2 π-Donor and -acceptor substituents. π Donors and acceptors influence the position of the bands to a larger extent than the σ-donor methyl group. On going from π-electron acceptor to π-electron donor substituents, the energy of the ^{1}LC increases from 30 110 to 33 660 cm^{-1} for [Re(CO)$_4$(dmdcb)]$^+$ and [Re(CO)$_4$(dmeob)]$^+$, respectively (see Table 1). The same trend is observed for the ^{3}LC energy (from 21 823 to 23 250 cm^{-1}, respectively). This trend is reproduced by the extended Hückel calculations (Fig. 8). The energy of the MLCT one-electron excitation follows this trend, but to a smaller extent, see Table 1.

The biggest influence of the substituents is on the π–π* singlet–triplet splitting when going from π-electron acceptor to π-electron donor substituents: from 6500 to 8600 cm^{-1} for [Re(CO)$_4$(dmdcb)]$^+$ and [Re(CO)$_4$(dmeob)]$^+$, respectively (see Table 1). The excited electron can delocalize better onto the substituent in a molecule containing an electron acceptor, as can be seen from the considerable electron density which is present on the substituents in the LUMO (Fig. 8). The change in the singlet–triplet splitting for MLCT excitations, on the other hand, is expected to be small.

The decrease in the π–π* singlet–triplet splitting on going from [Re(CO)$_4$(bpy)]$^+$ to [Re(CO)$_4$(dmdcb)]$^+$, is responsible for the decrease of ΔE from 7260 to 6490 cm^{-1}, respectively. This leads to an increase of the mixing coefficient α on adding the electron accepting dmdcb: 0.009 *vs*. 0.013, respectively (see Table 1). The influence of the electron donating dmeob is much smaller. This is due to a cancellation of effects which leaves ΔE and, as a consequence, the mixing coefficient more or less unchanged, see Table 1.

5 Conclusion

From this investigation on substituted cyclometallated and chelated rhenium(I) tetracarbonyl complexes and our earlier studies[13–16] we conclude that it is possible to influence the amount of MLCT character in the first excited $^3\pi$–π^* state only to a small extent. Cyclometallation has the largest effect,[16] increasing the MLCT character by a factor of 2. The influence of substitution with σ donors is negligible. π-Electron donors shift all transitions to higher energy, but they do not influence the ^{1}MLCT character in the lowest excited state. π-Electron acceptors decrease all transitions in energy and increase the MLCT character in the lowest energy state, but this effect is certainly smaller than the influence of cyclometallation.

The strong π-back bonding character of the CO ligands leads to an overall decrease of the metal orbital energies. The first ^{3}MLCT state therefore always lies above the first ^{3}LC state in tetracarbonylrhenium(I) complexes. Substituting a CO ligand by a Cl^- lowers the energy of ^{3}MLCT sufficiently for a ^{3}MLCT luminescence to be observed.[17] Tuning of this spectator ligand, as was done for a series of ruthenium(II) complexes,[39] appears to be the most efficient way to tune the excited state properties of rhenium(I) complexes over a large range. In order to achieve a competitive situation between ^{3}LC and ^{3}MLCT as emitting states, the π-back bonding characteristics of the spectator ligand must lie between those of CO and Cl^-. Acetonitrile is probably a good candidate for such a spectator ligand.

Acknowledgements

We thank C. Seidel for measuring some of the presented spectra, R. Basler, P. Egger, P. Franz, A. Loosli, P. Müller and K. Thoma for their help in solving the crystal structure, T. Armbruster and V. Malogajski for indexing the crystal faces and H. Weihe for fruitful discussions. Financial support by the Swiss National Science Foundation and the Hans-Sigrist Foundation is gratefully acknowledged. M. V. R. thanks the University of Hyderabad for leave.

References

1 A. Juris, V. Balzani, F. Barigeletti, P. Belser and A. von Zelewsky, *Coord. Chem. Rev.*, 1988, **84**, 85.
2 T. J. Meyer, *Acc. Chem. Res.*, 1989, **22**, 163.
3 O. Kohle, S. Ruile and M. Grätzel, *Inorg. Chem.*, 1996, **35**, 4779; R. Argazzi, C. A. Bignozzi, T. A. Heimer and G. J. Meyer, *Inorg. Chem.*, 1997, **36**, 2.
4 H. Hori, F. P. A. Johnson, K. Koike, O. Ishitani and T. Ibusuki, *J. Photochem. Photobiol. A*, 1996, **96**, 171.
5 B. O'Regan and M. Grätzel, *Nature* (*London*), 1991, **353**, 737.
6 M. T. Indelli, F. Scandola, I. Flamigni, J.-P. Collin, J.-P. Sauvage and A. Sour, *Inorg. Chem.*, 1997, **36**, 4247.
7 L. Karki and J. T. Hupp, *Inorg. Chem.*, 1997, **36**, 3318.
8 G. Frei, A. Zilian, A. Raselli, H. U. Güdel and H.-B. Bürgi, *Inorg. Chem.*, 1992, **31**, 4766.
9 M. G. Colombo and H. U. Güdel, *Inorg. Chem.*, 1993, **32**, 3081.
10 M. G. Colombo, A. Hauser and H. U. Güdel, *Inorg. Chem.*, 1993, **32**, 3088.
11 M. G. Colombo, A. Hauser and H. U. Güdel, *Top. Curr. Chem.*, 1994, **171**, 144.
12 M. G. Colombo, T. C. Brunold, T. Riedener, H. U. Güdel, M. Förtsch and H.-B. Bürgi, *Inorg. Chem.*, 1994, **33**, 545.
13 G. F. Strouse, H. U. Güdel, V. Bertolasi and V. Ferretti, *Inorg. Chem.*, 1995, **34**, 5578.
14 G. F. Strouse and H. U. Güdel, *Inorg. Chim. Acta*, 1995, **240**, 453.
15 F. W. M. Vanhelmont, G. F. Strouse, H. U. Güdel, A. C. Stückl and H. W. Schmalle, *J. Phys. Chem. A*, 1997, **101**, 2946.
16 F. W. M. Vanhelmont, H. U. Güdel, M. Förtsch and H.-B. Bürgi, *Inorg. Chem.*, 1997, **36**, 5512.
17 L. A. Worl, R. Duesing, P. Chen, L. Della Ciana and T. J. Meyer, *J. Chem. Soc., Dalton Trans.*, 1991, 849.
18 A. Juris, S. Campagna, I. Bidd, J.-M. Lehn and R. Ziessel, *Inorg. Chem.*, 1988, **27**, 4007.
19 A. R. Oki and R. J. Morgan, *Synth. Commun.*, 1995, **25**, 4093.
20 L. Della Ciana, W. J. Dressick and A. von Zelewsky, *J. Heterocycl. Chem.*, 1990, **27**, 163.
21 G. Maecker and F. H. Case, *J. Am. Chem. Soc.*, 1958, **80**, 2745.
22 R. J. Shaver and D. P. Rillema, *Inorg. Chem.*, 1992, **31**, 4101.
23 C. K. Johnson, ORTEP, Report ORNL-5138, Oak Ridge National Laboratory, Oak Ridge, TN, 1976.
24 CACAO, Computer Aided Composition of Atomic Orbitals, C. Mealli and D. Proserpio, *J. Chem. Educ.*, 1990, **67**, 399.
25 R. Hoffmann, *J. Chem. Phys.*, 1963, **39**, 1397.
26 A. Dedieu, T. A. Albright and R. Hoffmann, *J. Am. Chem. Soc.*, 1979, **101**, 3141.
27 E. V. Dehmlov and A. Sleegers, *Liebigs Ann. Chem.*, 1992, 953.
28 D. E. Lacky, B. J. Pankuch and G. A. Crosby, *J. Phys. Chem.*, 1980, **84**, 2068.
29 H. Riesen, L. Wallace and E. Krausz, *Mol. Phys.*, 1996, **87**, 1299.
30 E. Krausz and H. Riesen, *Comments Inorg. Chem.*, 1993,**14**, 323.
31 Y. Komada, S. Yamauchi and N. Hirota, *J. Phys. Chem.*, 1986, **90**, 6425.
32 H. Riesen, E. Krausz and L. Wallace, *J. Phys. Chem.*, 1992, **96**, 3621 and refs. therein.
33 M. Maestri, D. Sandrini, V. Balzani, U. Maeder and A. von Zelewsky, *Inorg. Chem.*, 1987, **26**, 1323.
34 A. P. Suisalu, A. L. Kamyshnyi, V. N. Zakharov, L. A. Aslanov and R. A. Avarmaa, *Chem. Phys. Lett.*, 1987, **134**, 617.
35 J. Michl and E. W. Thulstrup, *Spectroscopy with Polarized Light*, Verlag Chemie, New York, 1986, ch. 2.
36 F. O. Garces, K. A. King and R. J. Watts, *Inorg. Chem.*, 1988, **27**, 3464.
37 S. A. Fredericks, J. C. Luong and M. S. Wrighton, *J. Am. Chem. Soc.*, 1979, **101**, 7415.
38 F. W. M. Vanhelmont and H. U. Güdel, unpublished work.
39 K. Kalyanasundaram and Md. K. Nazeeruddin, *Chem. Phys. Lett.*, 1992, **193**, 292.

Received 8*th May* 1998; *Paper* 8/03465F